Journal of proteome research

Article

pubs.acs.org/jpr

Absolute Proteome Analysis of Colorectal Mucosa, Adenoma, and Cancer Reveals Drastic Changes in Fatty Acid Metabolism and Plasma Membrane Transporters

Jacek R. Wiśniewski,*[,†] Kamila Duś-Szachniewicz,[†,‡] Paweł Ostasiewicz,[‡] Piotr Ziółkowski,[‡] Dariusz Rakus,[§] and Matthias Mann[†]

[†]Department of Proteomics and Signal Transduction, Max-Planck-Institute of Biochemistry, Am Klopferspitz 18, 82152 Martinsried, Germany

[‡]Department of Pathology, Wrocław Medical University, 50-368 Wrocław, Poland

[§]Department of Animal Molecular Physiology, Wroclaw University, 50-205 Wrocław, Poland

Supporting Information

ABSTRACT: Colorectal cancer is a leading cause of cancer-related death. It develops from normal enterocytes, through a benign adenoma stage, into the cancer and finally into the metastatic form. We previously compared the proteomes of normal colorectal enterocytes, cancer and nodal metastasis to a depth of 8100 proteins and found extensive quantitative remodeling between normal and cancer tissues but not cancer and metastasis (Wiśniewski et al. PMID 22968445). Here we utilize advances in the proteomic workflow to perform an in depth analysis of the normal tissue (N), the adenoma (A), and the cancer (C). Absolute proteomics of 10 000 proteins per patient from microdissected formalin-fixed and paraffin-embedded clinical material established a quantitative protein repository of the disease. Between N and A, 23% of all proteins changed significantly, 17.8% from A to C and 21.6% from N to C. Together with principal component analysis of the patient groups, this suggests that N, A, and C are equidistant but not on one developmental line. Our proteomics approach allowed us to assess changes in varied cell size, the composition of different subcellular components, and alterations in basic biological processes including the energy metabolism, plasma membrane transport, DNA replication, and transcription. This revealed several-fold higher concentrations of enzymes in fatty acid metabolism in C compared with N, and unexpectedly, the same held true of plasma membrane transporters.

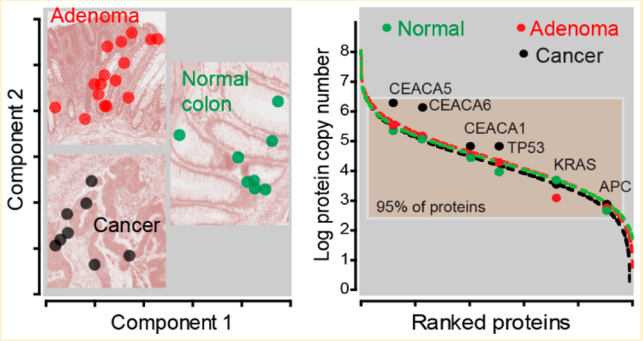

KEYWORDS: *colorectal cancer, adenomatous polyposis coli, enterocyte, metabolism, FFPE-tissue, quantitative proteomics, FASP, absolute protein quantification, total protein approach*

INTRODUCTION

Human colorectal cancer is the second leading cause of cancer-related death among adults in Europe.[1] In 2012 an estimated 446 800 new cases and 214 700 deaths occurred in 40 European countries. Colorectal cancer develops from the glandular epithelial tissue of the colon or rectum and involves an intermediate form, the colonic adenoma, which is a benign tumor of glandular epithelial tissue.[2] Colorectal adenomas are found in approximately one-third of asymptomatic patients before the age of 50 undergoing colonoscopy. These neoplasms are initially noninvasive, but within 10 to 20 years, in about 5% of patients, these adenomas progress into a cancer.[3] Thus, the adenoma−carcinoma sequence model, associated with the accumulation of multiple clonally selected genetic alterations, has been proposed to account for the gradual progression from normal tissue, via dysplastic epithelium to carcinoma.[4]

The idea of adenoma-carcinoma progression has been also supported by microarray analysis of gene expression or quantitative PCR-based assays, which enable simultaneous monitoring of the expression levels of multiple genes. Carvalho et al. examined genome-wide mRNA expression profiles of 37 colorectal adenomas and 31 colorectal carcinomas using oligonucleotide microarrays,[5] finding that mRNA expression of 248 genes was significantly different in carcinomas compared with adenomas, of which 96 were upregulated and 152 were downregulated. Gene ontology analysis revealed changes mainly in chromosome binding, chromosome segregation, mitosis, and the cell cycle. In addition, altered DNA methylation,[6] changes in microRNAs expressions,[7] and inflammation[8] are factors involved in the early development of colorectal neoplasia.

Received: June 5, 2015
Published: August 6, 2015

DOI: 10.1021/acs.jproteome.5b00523
J. Proteome Res. 2015, 14, 4005−4018

Molecular and genetic studies conducted since the 70s have demonstrated that the colorectal neoplastic transformation is related to alterations in the expression of genes controlling cell proliferation and apoptosis and increasing cell motility,[9,10] such as the oncogene *K-RAS*, the tumor suppressor genes *APC*, *DCC*, and *p53*, as well as DNA repair genes.[11−13] In 2007, Vogelstein and coworkers identified 140 candidate genes mutated in colorectal cancers by sequencing a panel of 11 colorectal neoplasias.[14]

Although studies like the ones cited above have provided important insights into many aspects of colorectal cancers, they do not yield direct information on the major active components of the cells, which are their proteins. A number proteomic studies have been performed in the past to fill this gap in understanding of the disease (reviewed in ref 15); however, there are very few large-scale and quantitative data sets describing the proteomes of the colorectal enterocytes (N), the adenoma (A), and cancer tissues (C). In 2012 we reported identification of 8100 proteins from normal, cancer, and metastatic tissue that had been laser-capture microdissected from formalin- and paraffin-embedded (FFPE) material.[16] Our analysis revealed extensive remodeling of the proteome between the normal and cancer cells and revealed 1700 statistically significant protein abundance changes. Very recently, using similar mass spectrometric technology, a large consortium of laboratories reported the identification of 7526 proteins in about 90 colorectal patient samples;[17] however, this study did not use microdissection and unfortunately these results were not compared with our study. Another newly published proteomic study on adenomatous lesions and normal mucosal samples[18] also measured a relatively large series of 30 samples but found a drastically lower percentage of statistically significant changes between N and A (212 of 4325 identified proteins), perhaps due to the relatively low depth of coverage in each sample and the absence of microdissection.

In the current study, we wished to employ advances in the proteomics workflow to focus on proteomic similarities and dissimilarities between the normal, benign neoplasm (adenoma), and cancer stages. We analyzed 16 laser microdissected adenoma patient samples and compared them with 8 samples of colon cancer tissues and patient-matched samples of the adjacent normal-appearing mucosa cells. We created a data set of 10 900 nonredundant protein groups of which we consistently quantified 8500 proteins. Expression levels of more than 2000 proteins are significantly altered between N and A, C and A, and C and N. We provide detailed analysis of tumor-related alterations either in the cell architecture, replication and transcription machineries, as well as energy metabolism.

MATERIALS AND METHODS

Formalin-Fixed Paraffin Embedded Human Tissue

Archival formalin-fixed and paraffin-embedded samples of adenoma and grade 2 or 3 of cancer were obtained from the Department of Pathology of Wrocław Medical University. Analysis of the samples followed an informed consent approved by the local ethics committee (no. KB-598/2011).

Tissue Microdissection and Lysis

Tissue was dissected with the Laser Pressure Catapulting (LPC) PALM Instrument (Zeiss, Göttingen, Germany) and lysed in a buffer consisting of 0.1 M Tris-HCl, pH 8.0, 0.1 M DTT, 0.5% (w/v) polyethylene glycol 20 000 and 4% SDS at 99 °C for 1 h as described[19] and visually demonstrated here.[20]

Determination of Total Protein and Peptide

Protein and peptide concentrations were assayed using the tryptophan fluorescence assay.[21]

Protein Digestion and Peptide Fractionation

Detergent was removed from the lysates, and the proteins were processed according to the MED-FASP protocol employing two consecutive steps of digestion with LysC and trypsin[22] using 30k filtration units (cat no. MRCF0R030, Millipore).[23] Peptides released by LysC and trypsin were fractionated into 4 and 2 SAX fractions, respectively.

LC−MS/MS Analysis

Peptides were separated over a C_{18} reverse-phase column (20 cm long, 75 μm inner diameter, in-house packed with ReproSil-Pur C_{18}-AQ 1.8 μm resin (Dr. Maisch, Ammerbuch-Entringen, Germany)) and were eluted with a linear gradient of 5−30% buffer B (80% ACN and 0.5% acetic acid) at a flow rate of 250 nL/min over 195 min. This was followed by 10 min of elution from 30 to 60% buffer B, a washout of 95% buffer B, and re-equilibration with buffer A. Peptides were electrosprayed and analyzed on a Q Exactive mass spectrometer using a data-dependent mode with survey scans acquired at a resolution of 50 000 at m/z 200 (transient time 256 ms). Up to the top 10 most abundant isotope patterns with charge ≥2 from the survey scan were selected with an isolation window of 1.6 Th and fragmented by HCD[24] with normalized collision energies of 25. The maximum ion injection times for the survey scan and the MS/MS scans were 20 and 60 ms, respectively. The ion target value for both scan modes was set to 10^6, meaning that most MS/MS scans accumulated ions to 60 ms. The dynamic exclusion was 25 s and 10 ppm. The performance of the mass spectrometer was checked on the weekly basis using BSA and whole HeLa cell lysate runs. All samples were separated on the same LC column. During the period of the analysis no observable changes in the LC performance were observed. The A, C, and N samples were analyzed in an alternate order: A1, A2, C1, N1, A3, A4, C2, N2; A5, A6, and so as to minimize potential effects related to column deterioration.

Data Analysis

The MS data were analyzed using the software environment MaxQuant[25] version 1.2.6.20 and its built-in Andromeda search engine.[26] Proteins were identified by searching MS and MS/MS data against the complete human proteome sequences from UniProtKB, version of May 2013, containing 88 820 sequences, respectively. Carbamido-methylation of cysteine was set as fixed modification and N-terminal acetylation and oxidation of methionine as variable modifications. Up to two missed cleavages were allowed. The initial allowed mass deviation of the precursor ion was up to 6 ppm, and for the fragment masses it was up to 20 ppm. Mass accuracy of the precursor ions was improved by time-dependent recalibration algorithms of MaxQuant. The "match between runs" option was enabled to match identifications across samples within a time window of 30 s of the aligned retention times. The maximum false peptide and protein discovery rates were set to 0.01. Protein matching to the reverse database or identified only with modified peptides were filtered out. Proteins identified with single peptides were likewise removed. Relative protein quantitation was performed using the LFQ algorithm of MaxQuant.[27] Two-sample *t*-test was applied for testing of differences in protein titers between sample groups: A/N, C/A, and C/N. Significance of outliers was calculated by multiple hypothesis testing[28] with the threshold value of 0.05. Protein

DOI: 10.1021/acs.jproteome.5b00523
J. Proteome Res. 2015, 14, 4005−4018

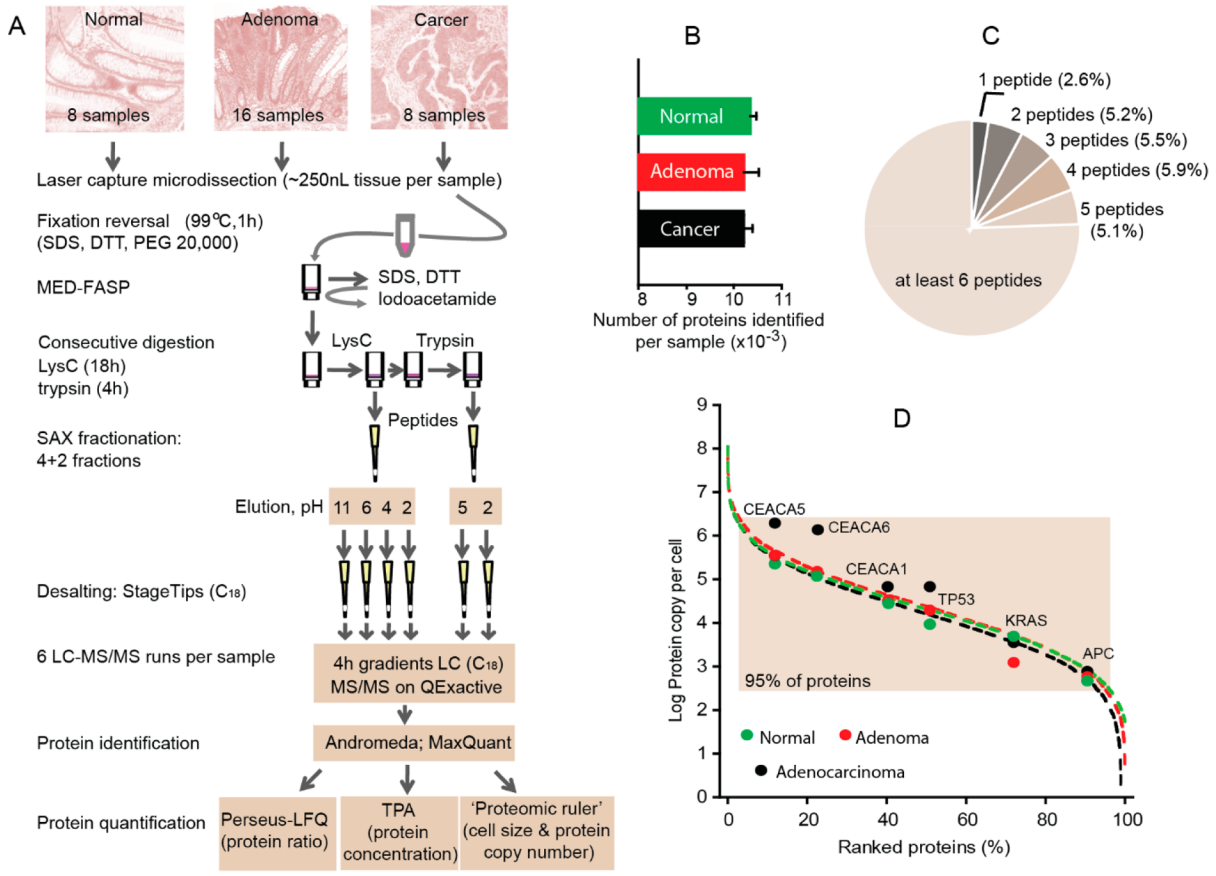

Figure 1. Proteomic analysis of FFPE archival samples of normal colonic mucosa, adenoma, and colorectal cancer. (A) Proteomic workflow applied to microdissected samples of normal colonic mucosa adenoma, and adenocarcinoma. (B) Number of proteins identified per sample. (C) Peptide based identification of proteins. (D) Distribution of protein abundances (copy numbers per cell) with selected examples of known proteins changed or with changed titers in cancer: CEA proteins, TP53, KRAS, and APC. Copy numbers were calculated using the "Proteome ruler" method.[30]

titers were calculated using the total protein approach (TPA)[16,29] using the relationships

Total protein (i):

$$\mathrm{TP}(i) = \frac{\mathrm{MS} - \mathrm{signal}(i)}{\text{total MS} - \mathrm{signal}}$$

or

Protein concentration (i):

$$C(i) = \frac{\mathrm{TP}(i)}{\mathrm{MW}(i)}\left[\frac{\mathrm{mol}}{\text{g total protein}}\right]$$

whereas the total protein content of the cells and the protein copy number per cells were assessed using the proteomic ruler approach assuming 6.5 pg as the DNA content of the 2n human cell:[30]

Total protein per nucleus:

$$TPn = 6.5 \times 10^{-12}\frac{\text{total MS} - \mathrm{signal}}{\mathrm{MS} - \mathrm{signal(total\ histone)}}\ [\mathrm{g}]$$

and Protein (i) copy number:

$$\text{copy number}\ (i) = N_A \times TPn \times C(i)$$

where N_A is the Avogadro constant. The calculations were performed in Microsoft Excel. The LC–MS/MS label-free protein quantitation platform applied was verified with Western blots in our recent publications.[31−33] Pathway analysis on LFQ data was performed using "Perseus" (http://www.perseus-framework.org/).

RESULTS

Identification of 10 900 Proteins from Laser Microdissected Normal Colonic Mucosa, Adenomas, and Adenocarcinoma

To compare the proteomes of the normal colonic (N), adenoma (A), and adenocarcinoma (C) cells, we analyzed archival formalin-fixed and paraffin-embedded material of 8 matched clinical samples of N and C and 16 nonmatched samples of A (Figure 1A) (SI Table 1). We used laser capture microdissection to obtain enriched populations of enterocytes, adenoma, and cancer cells. From each sample we collected a volume of ~250 nL of cells, which we processed using the FFPE-FASP procedure using consecutive sample digestion with LysC and trypsin.[34] Total peptide yields were 23.9 ± 4.4 μg per sample. To maximize depth of proteome coverage, LysC and tryptic peptides were fractionated by anion exchange chromatography into four and two fractions, respectively. Proteomic analysis was conducted by LC–MS/MS on a Q Exactive mass spectrometer (Figure 1A). The complete data acquisition took 32 days. In our analysis, 145 000 unique peptides corresponding to 10 900 proteins were identified at a false discovery rate (FDR) of 1% (SI Table 2). Protein ratios between the N, A, and C groups were assessed using the label free module of the MaxQuant software (LFQ).[27] Protein concentrations were calculated using the total protein approach,[16] and protein copies per cell were obtained using the

DOI: 10.1021/acs.jproteome.5b00523
J. Proteome Res. 2015, 14, 4005−4018

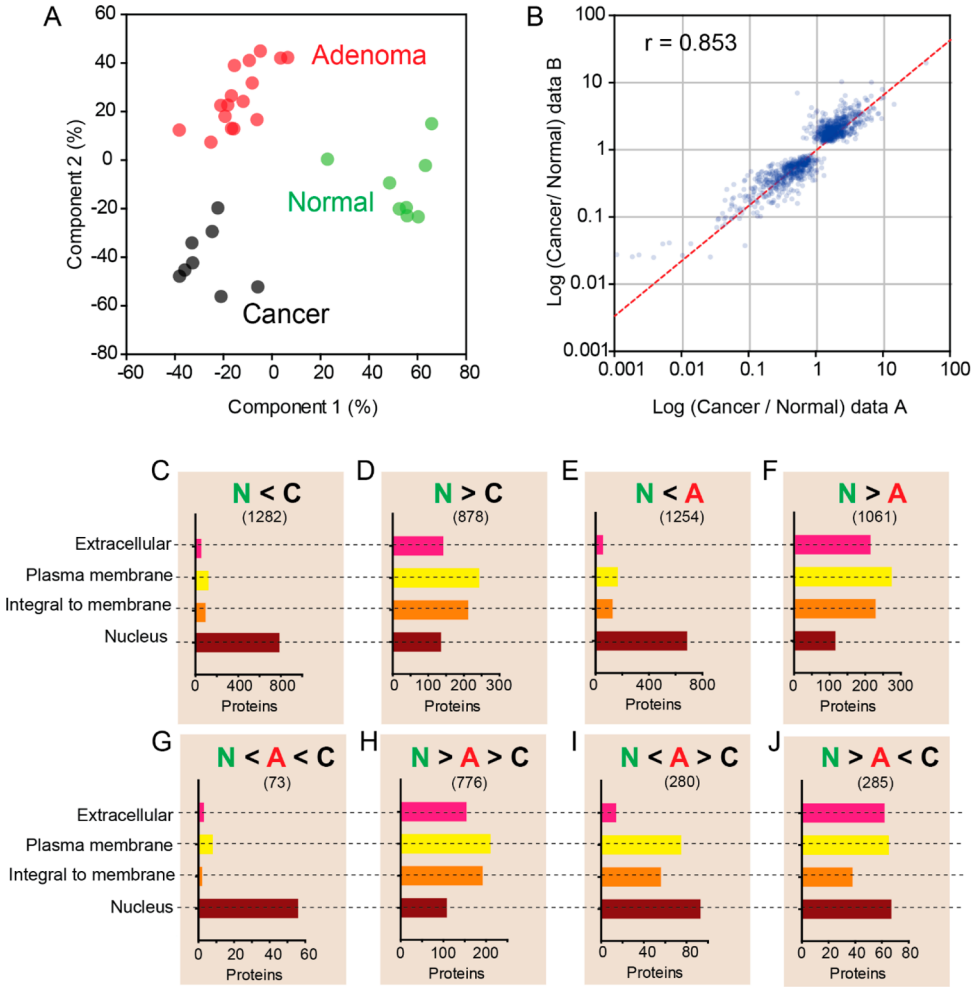

Figure 2. Statistical analysis of the data. (A) Principal component analysis. (B) Comparison of the cancer to normal ratios obtained for significantly changed protein abundances identified in this study and in the previously published data.[16] (C–J) Classification of the significantly changed protein abundances according to the observed change between N, A, and C according to their Gene Ontology annotation. > and < indicate decrease or increase in abundance, respectively. The values in parentheses indicate the number of outliers in each group.

Proteomic Ruler method.[30] In each of the samples 9700–10 500 proteins were identified (Figure 1B), and 97.4% of the proteins were identified by at least two peptides (Figure 1C). Remarkably, 75% of the proteins were identified with more than five peptides. The protein abundances expressed in copy number per cell spanned seven orders of magnitude, but the levels of 95% of the proteins were within a 10 000-fold titer range (Figure 1D). Proteins known as adenocarcinoma markers (CEA), as well as those originating from genes involved in the colon cancer etiology (TP53, KRAS, and APC), were identified within this range of abundance.

Statistical Analysis of the Data

A total of 8237 proteins that were identified in at least 75% of samples in each group, N, A, or C, were subject to calculation of protein ratios and subsequent statistical analysis. Principal component analysis (PCA) revealed clearly separated groups, with A and C separated in component 2 of the PCA, whereas both were about equidistant to the enterocytes (Figure 2A). *t*-test analysis allowed determination of the statistical significance of the protein differences. In total 2300, 1780, and 2161 proteins were significantly ($P < 0.05$) upregulated or downregulated between N/A, A/C, or N/C, respectively (SI Table 3). In our previous study,[16] 1801 proteins were statistically different between N/C, of which 1148 are identical to the A/C outliers found here (Figure 2B). Next, we classified the pairwise outliers according to their down- and upregulation between any two stages with respect to their subcellular locations (Figure 2C–F). The outliers that were upregulated in either the N/A or N/C pairs were to 50–60% composed of nuclear proteins, whereas they were rarely cell surface and membrane proteins (Figure 2C,E). In contrast, proteins downregulated in either the N/A or N/C pair were largely located in the extracellular region and in the cell membranes, whereas the contribution of nuclear proteins was markedly reduced (Figure 2D,F). When analyzing proteins changing within the N–A–C sequence we identified 285 and 280 that were, respectively, significantly down- or upregulated in adenoma (Figure 2G–J). A total of 776 and 76 proteins occurred in the adenoma stage at titers in between N and C (Figure 2G,H).

Extensive Alterations in Cell Composition and Function

The fact that at least 40% of proteins changed significantly in the combined data set of N, A, and C prompted us to investigate if the content of different subcellular compartments had changed between the stages. Taking a closer look at all proteins annotated for cell organelles, a comparison of the normal enterocytes (N) with the cancer cells (C) revealed a significant increase in the

DOI: 10.1021/acs.jproteome.5b00523
J. Proteome Res. 2015, 14, 4005–4018

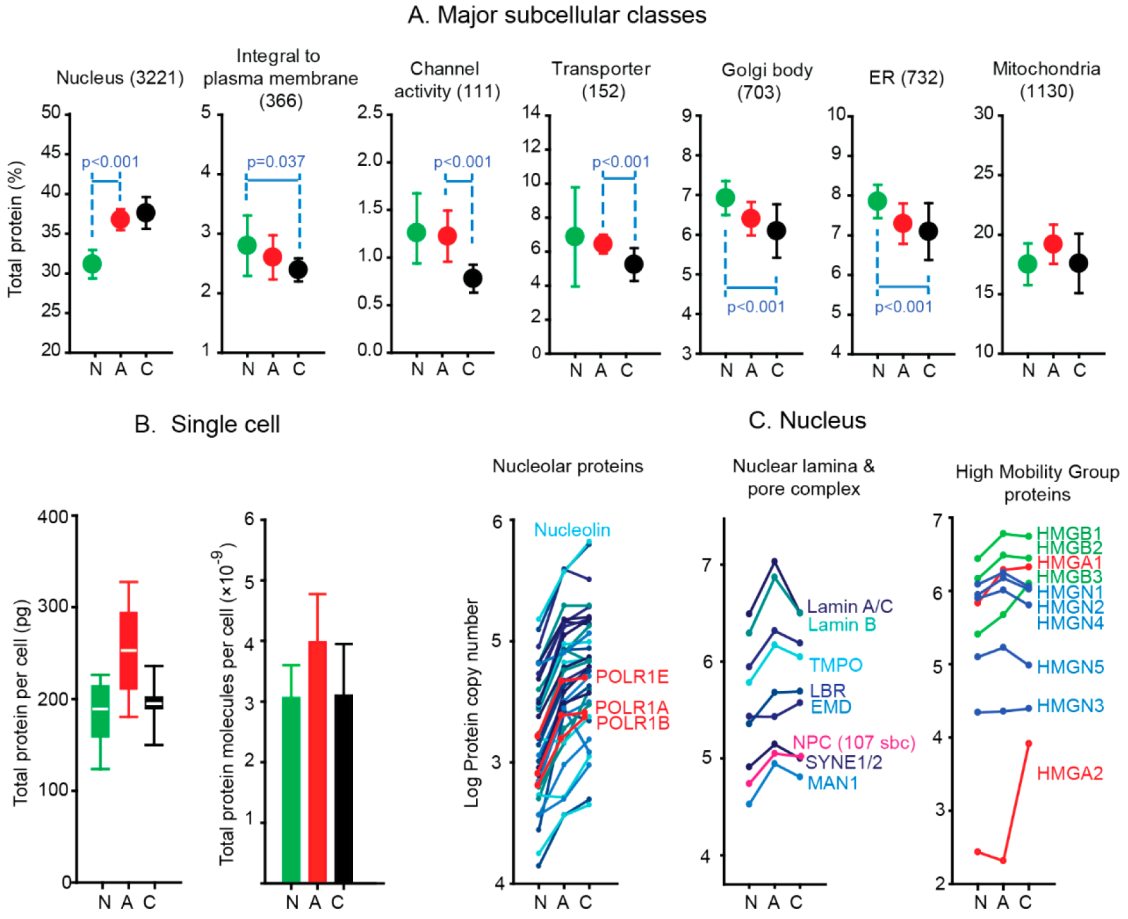

Figure 3. Global changes in organization the normal, adenoma, and cancer cells. (A) Abundance of all proteins matching selected subcellular locations. (B) Protein content of the cells. (C) Titer alterations of selected nuclear proteins with focus on nucleolus, nuclear lamina and the pore complex and the high mobility group proteins. 107 sbc, pore subcomplex NUP107.

overall protein fraction representing nuclear proteins ($p < 0.01$). In contrast, in cancer cells, the fractions of proteins of integral to plasma membrane, endoplasmic reticulum, and Golgi body were downregulated (Figure 3A). This was also well-reflected in the decreased abundance of channels and transporters (Figure 3A). Interestingly, we did not observe changes in the overall content of mitochondria between N and C. All of these observations are in a good agreement with the results of our previous study.[16] The subcellular composition of the adenoma cells, which was not analyzed in the previous study, was always in-between N and C; however, in the adenoma the content of nuclear proteins was similar to that in the cancer, and the contents of channel and transporter proteins were closer to the normal enterocytes than to the cancer cells.

We recently described a method termed "Proteome ruler", which employs the constant ratio between histones and cellular DNA to calculate the number of cells in a sample or the cell size.[30] Here we found that single enterocyte or cancer cells each contained about 180 pg total protein, while the adenoma cells were larger with 240 pg per cell (Figure 3B) (SI Table 4). These protein contents correspond to 3×10^9 protein molecules per one normal or cancer cell and 4×10^9 proteins in the adenoma cell. These values are close to the 4.8×10^9 values calculated in our previous study, where we, however, had to make assumptions for the cell size and the cellular protein concentrations.[16]

Next, we compared the abundances of proteins specific for nucleolus, nuclear membrane, and the high mobility group (HMG) proteins. The titer of the specific nucleolar protein showed common upregulation in A and C compared with N (Figure 3C). These data suggest a highest content of nucleoli in the cancer cells, which is in a good agreement with histopathological experience that relates increased number of nucleoli to increased aggressiveness of the cancer.[35]

The key components of the nuclear membrane are the nuclear lamina and the nuclear pore complex. Most of their proteins were about 2−4 fold upregulated from N to A, and only little changed between A and C (Figure 3C). A clear exception was the decrease in Lamins A/C and B. The proteins of the core subcomplex NUP107 of the nuclear pores occurred in A and C on average at 100 000 copies per nucleus. This value is similar to that recently reported for HeLa cells on the basis of targeted proteomics and synthetic standards.[36] Interestingly, our data suggest that the nuclei in normal enterocytes contain about half the nuclear pore complexes of A and C.

The HMG proteins are a heterogeneous group involved in various cellular processes, including modulation of transcription. Usually their abundance correlates with increased cell proliferation, and some of these proteins are unregulated in neoplasms.[37] Our proteomic analysis reflected this heterogeneous pattern with some proteins upregulated and others essentially unchanged (Figure 3C). One striking finding relates to the HMGA2 protein, which has been described as highly upregulated in colon cancer[38] and which we find to be more than 100 times upregulated, specifically in cancer.

DOI: 10.1021/acs.jproteome.5b00523
J. Proteome Res. 2015, 14, 4005−4018

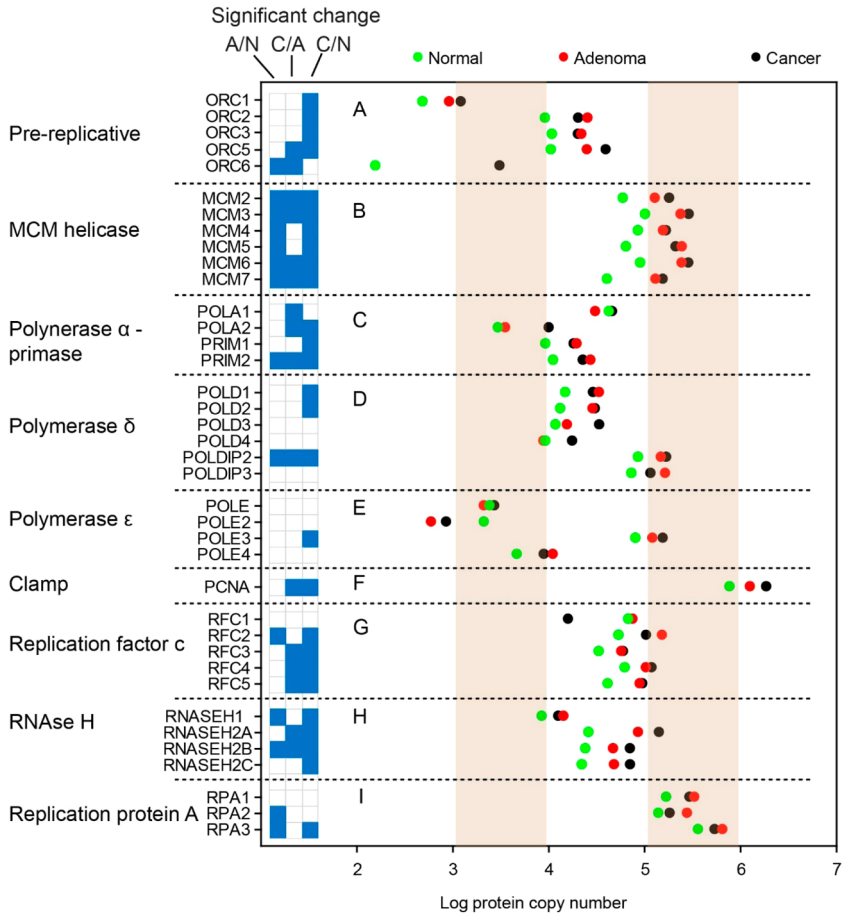

Figure 4. Modulation of replication in the normal−adenoma−adenocarcinoma sequence. Statistically significant changes between N/C, N/A, and C/A are indicated on the left as blue boxes.

The high number of identified proteins allowed systematic investigation of functional alterations characteristic for cancer and adenoma such as metabolic processes, solute transport, replication, and transcriptional regulation, among many others (SI Table 5). Below we provide a detailed picture some of these processes.

Extensive Alterations in the Machinery of the Cell Proliferation

In Figure 4 and all subsequent figures, we list the protein complex members on the vertical axis together with a grid designating the significance or otherwise of these changes. This is followed by the color-coded absolute expression values of the proteins in N, A, and C to give the reader an overview of both the absolute expression values and how these values change between the stages.

Sustaining proliferative signaling and replicative immortality are among to the hallmarks of cancer.[39] DNA replication commences by recruitment of ORC proteins to the origins of replication forming the prereplicative complex. This complex is composed of the core structure of ORC2, ORC3, ORC4, and ORC5 and the proteins ORC1 and ORC6 (ref 40). We observed a statistically significant 2-fold upregulation of ORC1, ORC2, ORC3, and ORC5 between the N and C samples, whereas, in respect to adenoma, ORC5 and ORC6 were significantly augmented in the cancer cells (Figure 4A).

In the next step of replication, the ORC complex attracts the helicase complex, which unwinds DNA. Once the replication fork is initiated, a large number of proteins bind to the single strands. The most prominent of them are the DNA polymerases that synthesize the new DNA by adding complementary nucleotides to the template strand. Previous work has shown that germline mutations of the genes *POLD1* and *POLE* coding for largest subunits DNA polymerases involved in the DNA replication predispose to 'polymerase proofreading associated polyposis' (PPAP), a disease characterized by multiple colorectal adenomas and carcinoma, with high penetrance and dominant inheritance. In addition, somatic mutations in *POLE* have also been found in sporadic colorectal and endometrial cancers.[41] Our study provides quantitative data on all of the canonical components of DNA replication machinery. We found that proteins that are known to be organized in complexes of defined stoichiometry have similar copy numbers. These include the minichromosome maintenance (MCM) helicase complex composed of six subunits MCM2−MCM7, heteropentamer replication factor c (RFC1-RCF5), and the single-stranded DNA-binding heterotrimer of the replication protein A (RPA1−RPA3). The subunits of the replication polymerases α, δ, and ε, each consisting of four subunits, do not follow such ordered stoichiometry. This may reflect hierarchal organization of their holoenzymes as well as involvement of these polymerases also in another process, such as DNA repair. In the functional complexes of the polymerases δ and ε, the holoenzymes are assembled together with the homotrimeric PCNA protein and the RCF pentamer. Considering the quaternary structures of these proteins, their copy numbers are similar.

DOI: 10.1021/acs.jproteome.5b00523
J. Proteome Res. 2015, 14, 4005−4018

In total, we identified 36 proteins of the core machinery of replication, 23 of which showed statistically significant changes, and 95% of the 36 proteins displayed continuously increasing abundance within the normal−adenoma−cancer sequence. Thus, our data reflect an amplification of the proliferative potential of the adenoma cells, which is further augmented in the cancer.

Changes in the Transcription Machinery

Increased proliferation requires elevation of the titers of signaling and metabolic proteins and hence the transcription and translation machineries. In humans there are three main systems that read the genetic information and produce RNAs. The RNA polymerase 1 synthesizes the 45S precursor of the rRNAs, the RNA polymerase 2 produces the pre-mRNAs, and the RNA polymerase 3 synthesizes tRNAs, rRNA 5S, and other small RNAs. Each of the polymerases is composed of several subunits, and their transcriptional activity is modulated by general and specific transcription factors. Our analysis allowed identification of more than 50 components of the basal transcriptional machinery, half of which changed significantly between at least one of the analyzed tissues (Figure 5). Most of the proteins occurred at highest copy numbers in the cancer or adenoma, and their abundance was lowest in the normal cells. Our quantitative data reflect the quaternary organization of the polymerases that are composed of a set of polymerase specific core subunits (Figure 5A−C) and a number of shared subunits (Figure 5D). The core subunits of each of the three polymerases occurred at similar copy numbers, whereas the common subunits were present at several fold higher titers. The core subunits of the polymerase II had $4.6−9.2 \times 10^4$ copies in the normal enterocytes and at $0.6−1.2 \times 10^5$ copies in cancer. These values are similar to our previous estimates[16] and are 3 to 5 times lower than those reported for HeLa cells.[42] The average abundances of the core subunits of the polymerase 2 were about five times higher than those of the core subunits of the polymerases 1 and 3. This proportion corresponds well with the fact that 15 000, 65 000, and 10 000 nascent transcripts are made by Polymerases I, II, and III in HeLa cells, respectively.[43,44]

In comparison with the polymerases, the abundances of the general transcription factor subunits 2 and 3 (GTF2 and GTF3) showed a less ordered picture (Figure 5E). The most abundant GTF 2s had $(1 \text{ to } 2) \times 10^5$ copies, whereas this value was always below 6×10^4 for GTF 3s. The abundances of the transcription activation factors (TAFs) span three orders of magnitude. The TATA-binding protein-associated factor 2N (TAF15) was, with $(0.5 \text{ to } 1) \times 10^5$ copies, the most abundant in this group of proteins, whereas the TATA-binding protein (TBP) itself was present in only 2000−8000 copies. This is ten-fold lower than the number reported for HeLa cells.[42]

Alteration of Glucose Degradation and Storage

A key hallmark of cancer cells is their high capacity to metabolize glucose, even in the presence of oxygen.[45,46] This phenomenon, known as the "Warburg effect",[47] usually correlates with overexpression of several glycolytic enzymes in cancers.[48−50]

In line with this, we found that the concentrations of most glycolytic enzymes were highest in C, but when comparing C and N, we observed statistically significant elevation only for phosphoglycerate kinase (PGK) (Figure 6A). More statistically significant changes were related to N-A and A-C transitions; however, in these cases there was not a single trend showing an increase or a decrease in the titers.

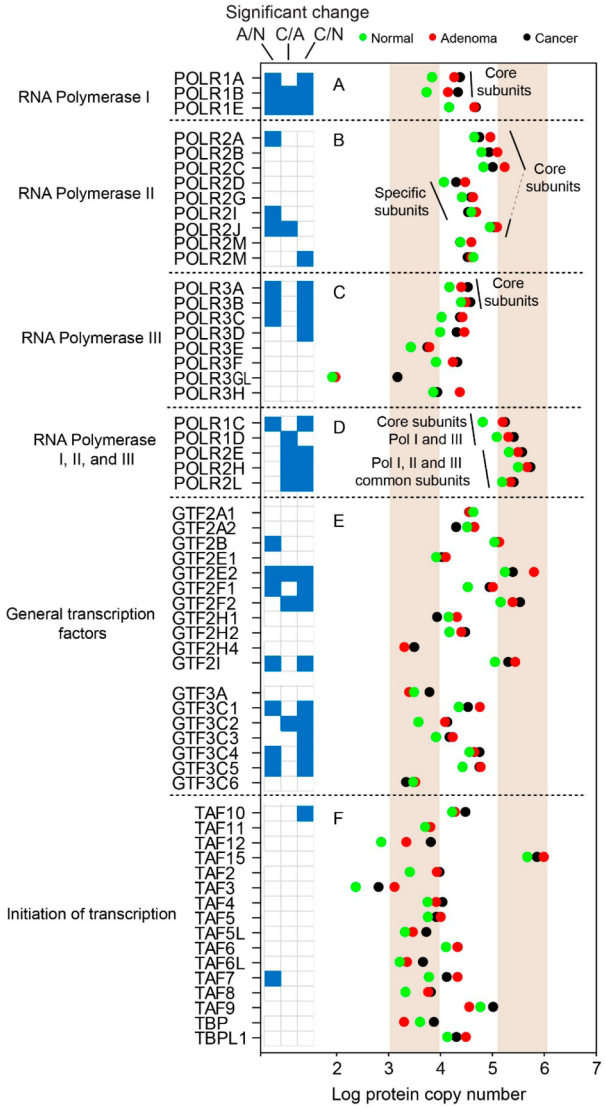

Figure 5. Alterations in general transcription processes between normal mucosa, adenoma, and adenocarcinoma. Statistically significant changes between N/C, N/A, and C/A were indicated on the left as blue boxes. (A) RNA polymerase I subunits, (B) RNA polymerase II subunits, (C) RNA polymerase III subunits, (D) shared subunits of the RNA polymerases, (E) general transcription factors, and transcription factors.

Previous studies have suggested that mRNA for glycolytic enzymes was enriched in A as compared with N and C.[51] In contrast, our results showed that the titers of glycolytic enzymes in A were not higher and were usually much lower than in C (Figure 6A). We also found that the expression of glycolytic proteins in A was not elevated as compared with that reported in N. In fact, the titer of a regulatory enzyme of glycolysis, phosphofructokinase (PFK), was the lowest in A. Evidently, the ability of A for glycolytic degradation of glucose does not represent an intermediate step between N−C during neoplastic transformation and presumably reflects a dysregulation of glycolytic pathway.

One of the most unexpected findings of our study was the lack of differences between N and C and A in the level of HK, an enzyme catalyzing the first irreversible reaction of glycolysis, which has been shown to be crucial for the proper functioning of biosynthetic pathways in lung and breast cancers and for cancer cell survival.[52] Our analysis suggests that the entry of glucose into

DOI: 10.1021/acs.jproteome.5b00523
J. Proteome Res. 2015, 14, 4005−4018

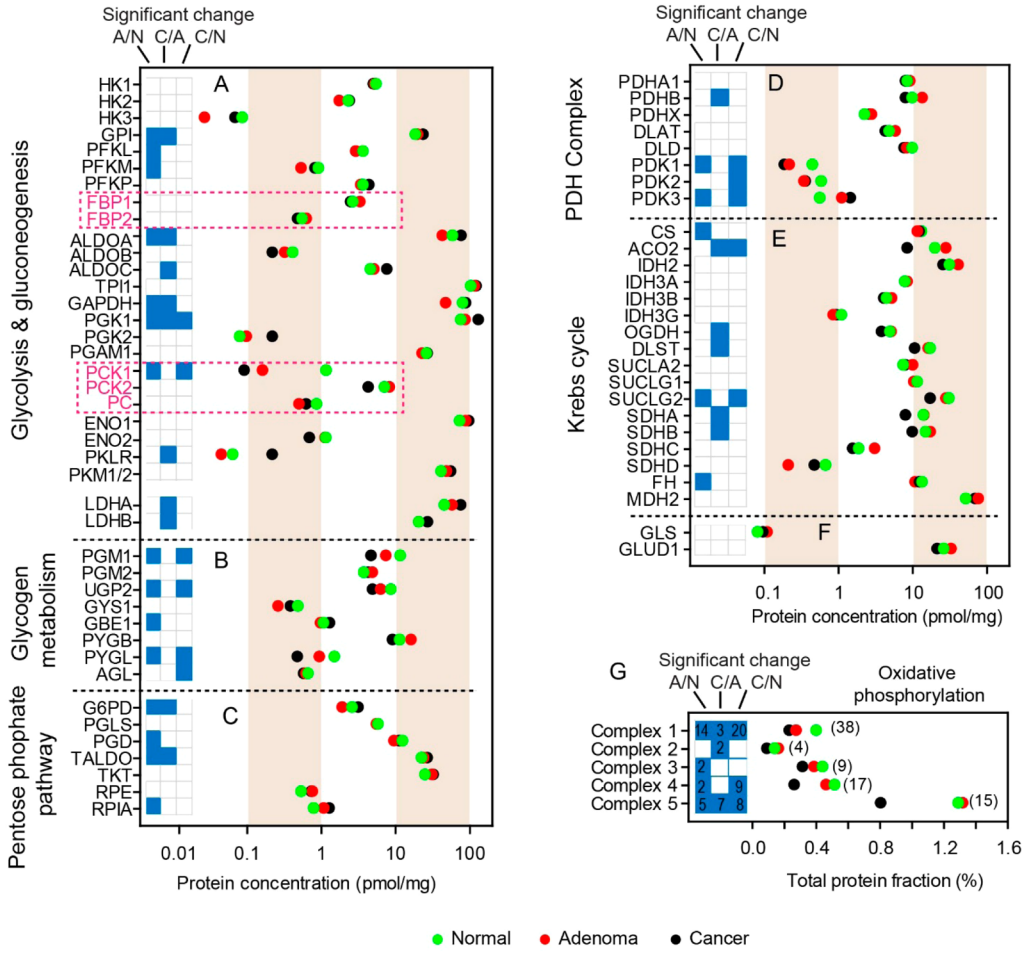

Figure 6. Variation in the energy metabolism processes upon normal to adenoma transition and the neoplastic transformation. Statistically significant changes between N/C, N/A, and C/A are indicated on the left as blue boxes. (A) Glycolysis and gluconeogenesis, (B) pentose phosphate pathway, (C) glycogen metabolism, (D) pyruvate dehydrogenase complex, (E) Krebs cycle, (F) glutamine transport and metabolism, and (G) oxidative phosphorylation. In G, the values are compiled fractions of total protein of components of individual complexes and the number of significantly altered proteins is given within the blue boxes.

cellular metabolism in C is regulated by the glucose membrane transporter, GLUT1 (SLC2A1), which is several times more abundantly expressed in C than in N (Figure 8). This corroborates previous findings that have associated neoplastic progression in the colon with increased GLUT1 glucose transporter expression.[53]

During the last years a line of evidence has been developed suggesting that down-regulation of fructose-1,6-bisphosphatase (FBP), a regulatory enzyme of gluconeogenesis, may be part of the mechanism responsible for increased glucose-to-lactate oxidation in cancer cells and may thus contribute to "the Warburg effect".[54−59] In contrast with those studies we did not observe a significant reduction of FBP concentration in C when compared with N (Figure 6A); however, the amount of FBP in A was elevated and was only 2 times lower than the amount of PFK, a glycolytic enzyme catalyzing the reverse of the FBP reaction. Thus, FBP may antagonize the glycolytic flux in adenoma cells.

The most substantial difference in the profiles of gluconeogenesis between the studied tissues concerned phosphophenolpyruvate carboxykinase (PCK), which converts oxaloacetate into phosphoenolpyruvate and is therefore a second regulatory enzyme of glucose synthesis from noncarbohydrates. The concentration of PCK was several times lower in C as compared with N and A (Figure 6A). This very substantial decrease in PCK titer has been previously observed[49] but its reasons remain enigmatic. We hypothesize that the lowering of PCK expression is a mechanism protecting oxaloacetate, the substrate of the enzyme, for synthetic activity in proliferating cells, where oxaloacetate may be a precursor for amino acids and nucleotide synthesis.

A commonly accepted idea is that colon mucosa and colorectal malignant cells accumulate glycogen, which then provides energy for cell proliferation.[60,61] It has also been speculated that elevated stores of glycogen may be a marker of malignancy as levels of glycogen had been found to increase with the malignancy of cancers and cancer-derived cells such as CaCo-2 cells.[62,63] Our analysis revealed, however, that the amounts of crucial enzymes of glycogen synthesis in the studied colorectal tissues were lowest in neoplastic cells (A and C) (Figure 6B), indicating that the capability for glycogen synthesis is not a hallmark of malignancy of colorectal cancers (Figure 6B); however, the titer of glycogen-degrading enzymes, glycogen phosphorylases (PYGB and PYGL), was also the lowest in C. This observation may explain our findings because it suggests that the malignant cells have an impaired glycogen degradation mechanism that may account for the previously observed accumulation of glycogen molecules in the cancer cells.[62,63]

DOI: 10.1021/acs.jproteome.5b00523
J. Proteome Res. 2015, 14, 4005−4018

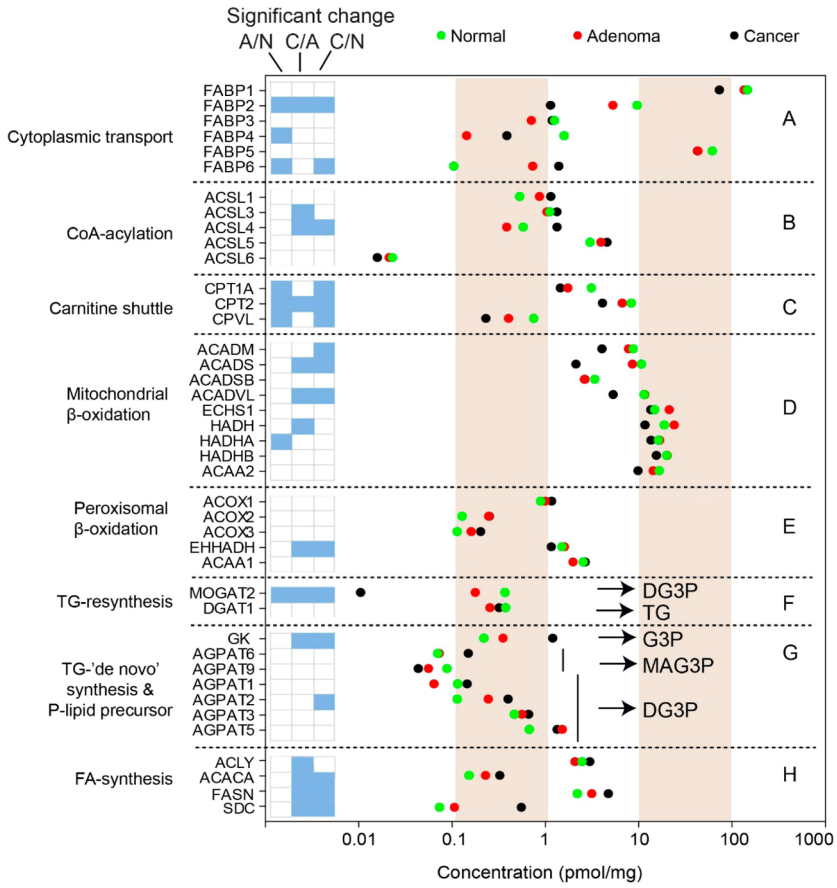

Figure 7. Fatty acid metabolism. Statistically significant changes between N/C, N/A, and C/A were indicated on the left as blue boxes. In the panels F and G, the intermediate and the final products of the triglyceride synthesis are indicated. DG3C, diacyl-glycerol-3-phosphate; TG, triglyceride; G3P, glycerol-3-phosphate; MAG3P, monoacyl-glycerol-3-phosphate. (A) Cytoplasmic transport, (B) CoA-acylation, (C) carnitine shuttle, (D) mitochondrial β-oxidation, (E) peroxisomal β-oxidation, (F) triglyceride resynthesis, (G) triglyceride "de novo" synthesis, and (H) fatty acid synthesis.

Glucose, apart from being oxidized in glycolysis or converted into glycogen, may serve as a substrate for the pentose phosphate pathway (PPP), which produces ribose, a precursor for nucleotides and NADPH, for the biosynthesis of glutathione used in the defense against oxidative stress. PPP is upregulated in proliferating cells, and an increased activity/expression of such PPP enzymes as glucose-6-phosphate dehydrogenase (G6PD), transketolase (TKT), and transaldolase (TALDO) is characteristic for several tissues and cells that have undergone neoplastic transformation.[64,65] Our findings concerning glucose metabolism in C are consistent with most of the previously published data. We found a significant increase in the titer of the regulatory enzymes of NADPH synthesis (G6PD) as well as of enzymes involved in the production of ribose precursors for nucleotides and nucleic acids (TKT and TALDO) (Figure 6C). The concentration of G6PD, the crucial enzyme of PPP, was highest in C and lowest in A (Figure 6C). In contrast, the amount of other PPP enzymes in A was similar to those of in C; however, the increase was statistically significant only when compared with N.

Oxidative Metabolism

The Krebs cycle is a series of reactions used to produce energy through oxidization of pyruvate-derived and fatty acids-derived Acetyl-CoA as well as amino acid-derived compounds such as fumarate, oxalacetate, α-ketoglutarate, and succinyl-CoA. Additionally, the Krebs cycle provides precursors for the biosynthesis of amino acids and the reducing agent NADH. Oxidative phosphorylation (OXPHOS) is the pathway in which the Krebs cycle-derived NADH and succinate is oxidized to reform ATP from ADP.

Analyzing the Krebs cycle and OXPHOS, we found that the ability of C to oxidize acetyl-CoA, as implied by the corresponding enzyme levels, was significantly lower than that of normal mucosa (Figure 6D,E). Previous studies have found reduced levels in C of Krebs cycle enzymes such as aconitase 2 (ACO),[66] succinate dehydrogenase (SDH),[67] and reduced activity of isocitrate dehydrogenase 1 (IDH).[68] Using the HCT116 cell line model, it has been also shown that neoplastic transformation of colorectal mucosa correlates with down-regulation of mitochondrial ATP synthase subunits (complex V of OXPHOS).[69] Compared with those studies, we found that in addition to down-regulation of ACO and the IDH and SDH complexes (SDH and succinate-CoA ligase (SUCL)) (Figure 6E) and complex V (Figure 6G), the abundance of proteins making up all complexes of OXPHOS was significantly reduced in C as compared with N (Figure 6G). The level of OXPHOS proteins in A, except those of complex II (succinate dehydrogenase complex), was lower than in N (Figure 6G). This suggests that the inhibition of OXPHOS may be one of the hallmarks of the N to A transition. Unexpectedly, we found that the amount of the majority of the Krebs cycle proteins, especially those thought to be down-regulated in cancers (ACO, IDH, SDH complex), was higher in A than in N (Figure 6E).

DOI: 10.1021/acs.jproteome.5b00523
J. Proteome Res. 2015, 14, 4005−4018

It has recently been shown that glutamine is the main source of both Krebs cycle-derived intermediates for fatty acid and amino acids synthesis for ATP production in cancer cells.[70−72] In line with this, we found that the main glutamine transporter, SLC7A5, was significantly more abundantly expressed in C than in N and A (Figure 8). Conversely, the titers of enzymes converting glutamine into α-ketoglutarate, a Krebs cycle intermediate, were similar in all colorectal stages (Figure 6F). From this, it might be concluded that the transport into a cell is a limiting step in glutamine metabolism in C.

Fatty Acid Metabolism

It is well-documented that increased proliferation rates have to be accompanied by upregulated intake of extracellular fatty acids (FAs) or their increased synthesis in cells. In comparison with the carbohydrate-metabolism-related alterations in cancer, those of FA metabolism have received less attention; however, their importance is increasingly recognized.[73] Our data provides in-depth insights into the alterations of components of the FA metabolism in the N−A−C sequence, as described later (Figure 7).

Cellular pools of FA and their CoA-esters are bound to FA binding proteins (FABPs), and we here identified six FABPs. Five isoforms of FABP were downregulated in A and C, whereas isoform 6 was significantly upregulated in A and C (Figure 7A). The biological meaning of this effect remains obscure because specific functions of the individual FABPs have not yet been elucidated.[74]

Acylation of FA with CoA is required for both the oxidative degradation and as well as for the synthesis of di- and triglycerides. Among the five FA-CoA ligases, (ACSL), four were at highest concentrations in C; however, only ACSL4 was statistically significantly upregulated (Figure 7B). This observation agrees well with the previously reported increase of ACSL4 in A.[75] If this alteration has any biological consequence remains questionable, however, because isoform 5 is several times more abundant and isoforms 1 and 3 occur at similar titers.

The β-oxidation of FAs occurs along the mitochondrial and the peroxisomal pathways. In the mitochondrial pathway, FAs with backbones of 16 carbons and lower are processed, whereas in the peroxisomes longer FAs are oxidized. In the small intestine[33] and in liver (our unpublished results), the concentrations of the enzymes of both pathways are similar in the colorectal tissues. In contrast, in colon we observed that the mitochondrial β-oxidation is prevailing (Figure 7D,E). The abundances of all enzymes of the mitochondrial pathway were downregulated in cancer and were unchanged between N and A (Figure 7D). The components of the mitochondrial shuttle of FA-CoA had similar alterations, indicating a coupling of the FA-CoA supply and FA β-oxidation in the mitochondria (Figure 7C).

Triglycerides undergo esterification into the glycerol derivatives in two ways, the "de novo" pathway, which initiates with the coupling of FA to glycerol-3-phosphate (G3P), and the "resynthetic" one, using monoacylglycerol incorporated from the extracellular space. Whereas proteins involved in the latter mechanism were most abundant in the normal mucosa cells (Figure 7F), those of the former one were most abundant in C (Figure 7G). The diacyl-G3P produced in this process is further used for phospholipid synthesis.

Finally, we observed a common increase in the titers of the enzymes of FA synthesis in A and C, the ATP citrate lyase (ACLY), acetyl-CoA carboxylase (ACC), fatty acid synthase (FASN), FA-CoA ligases (ACSL), as well as FA desaturase (SDC) (Figure 7B,H). In conclusion, our data provide a comprehensive picture of cancer-related alterations, which had in many but not all cases been observed separately for each of these proteins previously.[73]

Plasma Membrane Transporters

In this study we identified more than 100 plasma membrane proteins, which are involved in absorption of nutrients, xenobiotics, drugs, and salts (SI Table 1). Of those, 27 proteins had significantly changed expression between N and C, A and C, or N and C (Figure 8). In the cancer cells, transporters, which

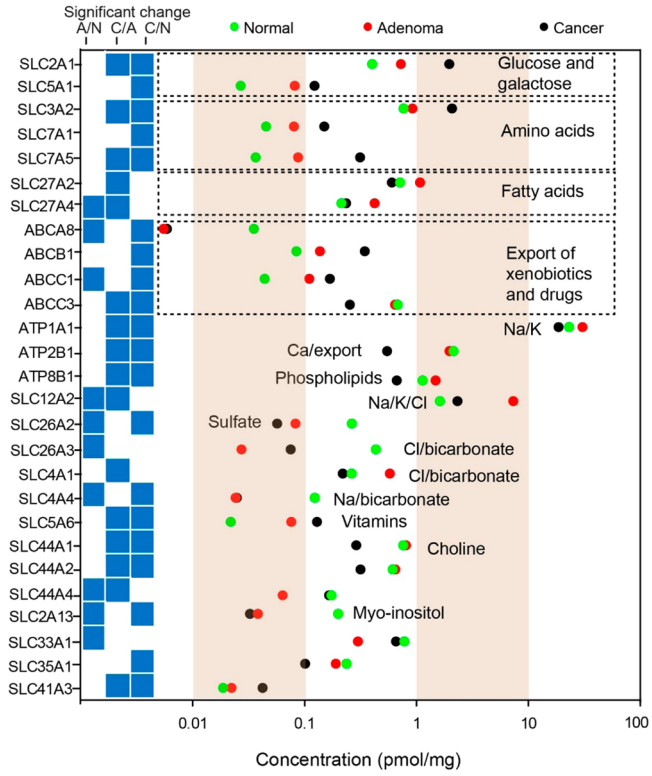

Figure 8. Concentrations of plasma membrane transporters with significantly different expression. Statistically significant changes between N/C, N/A, and C/A were indicated on the left as blue boxes. The solutes transported by the proteins are indicated.

mediate absorption of sugars (SLC2A1 and SLC5A1) and amino acids (SLC3A2, SLC7A1, and SCLC7A5), were present at concentrations several times higher than in the normal tissue and the adenoma. The increase in sugar absorption relates to the increased anaerobic metabolism in the cancer cells described above (Warburg effect[47]). Elevated transport of amino acid may reflect increased proteins synthesis or metabolism in the cancer cells. The titers of the fatty acid transporters (SLC27A2 and SLC27A4) were highest in A, whereas their expression remained nearly unaltered between C and N. The up-regulation of these transporters correlates well with the elevated levels of several enzymes of the beta-oxidation process (see preceding section).

The titers of the xenobiotic and drug efflux transporters were either up- or downregulated between N, A, and C (Figure 8). In the cancer cells, the multidrug resistance protein 1 (ABCB1) and the multidrug resistance-associated protein 1 (ABCC1) were strongly upregulated, whereas the titer of the ABCC3 protein, the most abundant efflux transporter in the normal tissue, was attenuated in C.

DOI: 10.1021/acs.jproteome.5b00523
J. Proteome Res. 2015, 14, 4005−4018

Across the variety of proteins involved in ion exchange, their highest concentrations were almost always found in the normal tissue (Figure 8). In the majority of the cases, this presumably reflects the loss of electrolyte resorption function of the neoplastically transformed cells. The titers of the Na-dependent multivitamin transporter (SLC5A6), transporting biotin, and panthothenate were highest in the cancer cells. Both substances have a number of functions related to cell metabolism. Panthothenate is essential in CoA synthesis, whereas biotin functions as prosthetic group of many enzymes. The increased need for these substances in the metabolically very active cancer cells correlates well with the upregulation of the corresponding transporters.

DISCUSSION

In the past decade, tremendous efforts have been performed to identify novel markers for diagnosis and prognosis of colorectal cancer. In this process the role of proteomics has remained secondary, although many potential biomarkers have been reported[15] and proteins with possible disease driver functions have been identified.[17] An important development that proteomics has contributed in recent years is its ability to study clinical samples to a depth that is similar to that of microarrays[16] and even to next-generation sequencing technologies.[76]

In our previous work on colon cancer, we identified 1800 proteins with significantly changed titers between the cancer cells and normal enterocytes.[16] This number is similar to the more comprehensive analysis reported in this paper that allowed identification of 2100 significantly changed proteins between N and C. Notably, 1148 of these match those of the previous study and, importantly, have similar protein titer ratios, as indicated in Figure 2. In addition, both our previous[16] and the present studies also identified significant upregulation of hepatocyte nuclear factor 4 (NHF4A), outer mitochondrial membrane translocase 4 (TOMM34), and the proto-oncogene SRC kinase (SRC). These proteins were recently described as cancer driver candidates identified from 3899 genes products, whose abundance was quantified across 90 cancer patient samples.[17]

In the present study, we focus on the proteome of the benign precursor of the colorectal cancer, the adenoma, which we had not previously analyzed. Comparison of the proteomes of 16 adenoma samples with normal tissue led to identification of 2300 proteins with titers that were significantly changed between the diseased (A/C ratio) or healthy appearing cells (A/N ratio). These widespread changes are accompanied by a global cellular remodeling, extensive alterations in the energy metabolism pathways, and the machineries of cell replication and transcription, which are recorded here for the first time. As mentioned in the Introduction, a recent study comparing 30 normal and adenoma samples reports identification of only 212 significant protein changes.[18] Nonetheless, our data confirm the key observation of those authors, namely, the overexpression of the sorbitol dehydrogenase in adenoma. The alterations of the top 10 significant hits of that study are also in excellent agreement with our data, as 9 of them were found as significantly changing in the present work. The differences in the number of identified N to A alterations between the recent study and our work may be attributed to the applied technology. Whereas Uzozie et al.[18] prepared protein lysates from whole tissues, separated peptides by isoelectric focusing (OFFGEL) and used 8-plex iTRAQ for relative quantification, in our study, protein lysates were prepared from microdissected cells, peptides were generated and fractionated by MED-FASP-SAX, and the quantification was label free. Clearly, the analysis of homogeneous cell populations, using simpler peptide separation and label-free quantification used in our study, lead to the better proteomic depth and allowed identification of several fold larger number of proteins with significantly changed titers.

Whereas adenomas are benign, their transformation to cancer is associated with a high risk of metastases and subsequent death. Clinical data have shown that early diagnosis and treatment of colon cancer significantly reduces mortality rates. For this reason, knowledge of specific cancer-associated proteins, especially adenoma-tumor associated proteins, is critical to identify effective methods for noninvasive diagnosis and monitoring of colorectal cancer. In contrast with the majority of studies using clinical material, the present work did not aim at identification of potential biomarkers. Nevertheless, our data now provide new insights into the proteome alterations accompanying cellular transformation. We identified 1780 significant changes in the adenoma to cancer comparison, and 429 of these alterations were unique to the adenoma−cancer sequence. This large number suggests that the mere characterization of a protein as significantly changing between stages of cancer development is not sufficient to qualify as a genuine and specific biomarker.

As an alternative to biomarker studies, we here generated a very deep reference data set encompassing proteomes of normal colon and its neoplastic diseases. Instead of seeking proteins that can be specifically associated with tumor and cancer commencement to detect or monitor the disease, we here characterized at the whole proteome level the basic cellular and physiological processes underlying the neoplasm and malignant transformation.

Such global quantitative description of cancer metabolism as reflected in the absolute abundance of the enzymes involved enables a deeper insight into the biology of cancer tissue, and it also reduces the number of hypothetical targets to be studied in the context of cancer prevention. For example, several studies have investigated the upregulation of various isoforms of glycolytic enzymes (such as ALDOA, GAPDH, ENO1, and PKM2) in the context of the Warburg effect in colorectal cancer (reviewed in ref 15) and suggested that these proteins represent a potential target for the prevention or treatment of the disease.[50] Our study reveals, however, that the expression of glycolytic enzymes in colorectal adenoma and carcinoma does not undergo significant changes, whereas the only protein that appears to be involved in the observed stimulation of glucose metabolism in these neoplastic tissues is the glucose transporter, SLC2A1. The other mechanism that is presumably responsible for the observed elevation of glycolytic flux and lactate production in colorectal cancer is a decreased ability of the PDH complex to convert pyruvate to acetyl-CoA as well as a significantly lowered abundance of mitochondrial enzymes that oxidize Acetyl-CoA to H_2O and CO_2 (Krebs cycle and OXPHOS). Importantly, the decrease in Krebs cycle proteins and OXPHOS does not correlate with significant changes in the titer of total mitochondrial proteins, suggesting that mitochondria-associated metabolism, but not glycolysis, undergoes strong rearrangement during neoplastic transformation.

ASSOCIATED CONTENT

Supporting Information

The Supporting Information is available free of charge on the ACS Publications website at DOI: 10.1021/acs.jproteo-

DOI: 10.1021/acs.jproteome.5b00523
J. Proteome Res. 2015, 14, 4005−4018

me.5b00523. The mass spectrometry proteomics data have been deposited to the ProteomeXchange Consortium[77] via the PRIDE partner repository with the data set identifier PXD002137.

SI Table 1: Sample origin, patient sex and age, and cancer grade and adenoma type. (PDF)

SI Table 2: List of all identified proteins with their cellular titers and copy numbers. (XLSX)

SI Table 3: Statistical analysis of the LFQ data. (XLSX)

SI Table 4: The "proteomic ruler"-based calculation of the total protein content per cell. (XLSX)

SI Table 5: Pathway analysis using the KEGG Pathway annotations. (XLSX)

AUTHOR INFORMATION

Corresponding Author

*Tel: +49 89 8578 2205. E-mail: jwisniew@biochem.mpg.de.

Notes

The authors declare no competing financial interest.

ACKNOWLEDGMENTS

We thank Korbinian Mayr for assistance in mass spectrometric analysis and Katharina Zettl for technical assistance. This work was supported by the Max-Planck Society for the Advancement of Science and the Polish National Center of Science (DEC-2011/01/N/NZ5/04253).

ABBREVIATIONS

A, adenoma; ABCB1, multidrug resistance protein 1; ABCC1, multidrug resistance-associated protein 1; ABCC3, ABCC3 protein; ACC, acetyl-CoA carboxylase; ACLY, ATP citrate lyase; ACO63, aconitase 2; ACSL, fatty acid-CoA ligases; ACSLs, fatty acid-CoA ligases; ALDOA, fructose-bisphosphate aldolase A; *APC*, *Adenomatous polyposis coli*; APC, adenomatous polyposis coli protein; BSA, bovine serum albumin; C, cancer; CEA, carcinoembryonic antigen; CRC, colorectal cancer; *DCC*, *netrin receptor DCC*; DTT, dithiothreitol; ENO1, alpha-enolase; FABPs, fatty acids binding proteins; FAs, fatty acids; FASN, fatty acid synthase; FBP, fructose-1,6-bisphosphatase; FDR, false discovery rate; FFPE tissue, formalin-fixed and paraffin-embedded tissue; G3P, glycerol-3-phopshate; G6PD, glucose-6-phosphate dehydrogenase; GAPDH, glyceraldehyde-3-phosphate dehydrogenase; GLUT1 (SLC2A1), glucose membrane transporter 1; GTF2, general transcription factor subunits 2; GTF3, general transcription factor subunits 3; HCD, higher-energy collisional dissociation; HMG proteins, high mobility group proteins; HMGA2, high mobility group protein HMGI-C; IDH65, isocitrate dehydrogenase 1; *K-RAS*, *GTPase KRas*; LC column, liquid chromatography column; LC–MS/MS, liquid chromatography–tandem mass spectrometry; LFQ, label-free Quantitation; lpc, laser pressure catapulting; MCM, minichromosome maintenance; MCM2, minichromosome maintenance complex component 2; MCM7, minichromosome maintenance complex component 2; MED-FASP, multienzyme digestion-filter-aided sample preparation; MS/MS, tandem mass spectrometry; N, normal colorectal enterocytes; NADH, nicotinamide adenine dinucleotide (reduced form); NADPH, nicotinamide adenine dinucleotide phosphate-oxidase; NHF4A, hepatocyte nuclear factor 4; NUP107, nuclear pore complex protein Nup107; ORC1–ORC6, origin recognition complex, subunit 1–6; OXPHOS, oxidative phosphorylation; *p53*, *cellular tumor antigen p53*; PCA, principal component analysis; PCK, phosphophenolpyruvate carboxykinase; PCNA, proliferating cell nuclear antigen; PCR, polymerase chain reaction; PFK, phosphofructokinase; PGK, phosphoglycerate kinase; PKM2, pyruvate kinase; POLD1, DNA polymerase delta catalytic subunit; POLE, DNA polymerase epsilon catalytic subunit A; PPP, pentose phosphate pathway; PYGB, glycogen phosphorylase, brain form; PYGL, glycogen phosphorylase, liver form; RFC1–RCF5, heteropentamer replication factor c; RPA1–RPA3, single-stranded DNA-binding heterotrimer of the replication protein A; SAX, strong anion exchange; SDC, fatty acid desaturase; SDH64, succinate dehydrogenase; SLC27A2, very long-chain acyl-CoA synthetase; SLC27A4, long-chain fatty acid transport protein 4; SLC2A1, Solute carrier family 2; SLC3A2, 4F2 cell-surface antigen heavy chain; SLC5A1, solute carrier family 5 (sodium/glucose cotransporter), member 1; SLC5A6, Na-dependent multivitamin transporter; SLC7A1, high affinity cationic amino acid transporter 1; SLC7A5, large neutral amino acids transporter small subunit 1; SLC7A5, large neutral amino acids transporter small subunit 1; SRC, proto-oncogene SRC kinase; SUCL, succinate-CoA ligase; TAF15, TATA-binding protein-associated factor 2N; TAFs, transcription activation factors; TALDO, transldolase; TKT, transketolase; TOMM34, outer mitochondrial membrane translocase 4; TPA, total protein approach; TP53, cellular tumor antigen p53

REFERENCES

(1) Ferlay, J.; Steliarova-Foucher, E.; Lortet-Tieulent, J.; Rosso, S.; Coebergh, J. W.; Comber, H.; Forman, D.; Bray, F. Cancer incidence and mortality patterns in Europe: estimates for 40 countries in 2012. *Eur. J. Cancer* **2013**, *49*, 1374–1403.

(2) Fearon, E. R.; Vogelstein, B. A genetic model for colorectal tumorigenesis. *Cell* **1990**, *61*, 759–767.

(3) Cattaneo, E.; Laczko, E.; Buffoli, F.; Zorzi, F.; Bianco, M. A.; Menigatti, M.; Bartosova, Z.; Haider, R.; Helmchen, B.; Sabates-Bellver, J.; Tiwari, A.; Jiricny, J.; Marra, G. Preinvasive colorectal lesion transcriptomes correlate with endoscopic morphology (polypoid vs. nonpolypoid). *EMBO molecular medicine* **2011**, *3*, 334–347.

(4) Leslie, A.; Carey, F. A.; Pratt, N. R.; Steele, R. J. The colorectal adenoma-carcinoma sequence. *Br. J. Surg.* **2002**, *89*, 845–860.

(5) Carvalho, B.; Sillars-Hardebol, A. H.; Postma, C.; Mongera, S.; Droste, J. T. S.; Obulkasim, A.; van de Wiel, M.; van Criekinge, W.; Ylstra, B.; Fijneman, R. J.; Meijer, G. A. Colorectal adenoma to carcinoma progression is accompanied by changes in gene expression associated with ageing, chromosomal instability, and fatty acid metabolism. *Cell. Oncol.* **2012**, *35*, 53–63.

(6) Beggs, A. D.; Jones, A.; El-Bahwary, M.; Abulafi, M.; Hodgson, S. V.; Tomlinson, I. P. Whole-genome methylation analysis of benign and malignant colorectal tumours. *Journal of pathology* **2013**, *229*, 697–704.

(7) Chai, J.; Wang, S.; Han, D.; Dong, W.; Xie, C.; Guo, H. MicroRNA-455 inhibits proliferation and invasion of colorectal cancer by targeting RAF proto-oncogene serine/threonine-protein kinase. *Tumor Biol.* **2015**, *36*, 1313.

(8) Chung, Y. C.; Chang, Y. F. Significance of inflammatory cytokines in the progression of colorectal cancer. *Hepato-Gastroenterology* **2003**, *50*, 1910–1913.

(9) Nathke, I. Relationship between the role of the adenomatous polyposis coli protein in colon cancer and its contribution to cytoskeletal regulation. *Biochem. Soc. Trans.* **2005**, *33*, 694–697.

(10) Pollock, C. B.; Shirasawa, S.; Sasazuki, T.; Kolch, W.; Dhillon, A. S. Oncogenic K-RAS is required to maintain changes in cytoskeletal organization, adhesion, and motility in colon cancer cells. *Cancer Res.* **2005**, *65*, 1244–1250.

(11) Bodmer, W. F.; Bailey, C. J.; Bodmer, J.; Bussey, H. J.; Ellis, A.; Gorman, P.; Lucibello, F. C.; Murday, V. A.; Rider, S. H.; Scambler, P.;

DOI: 10.1021/acs.jproteome.5b00523
J. Proteome Res. 2015, 14, 4005–4018

et al. Localization of the gene for familial adenomatous polyposis on chromosome 5. *Nature* **1987**, *328*, 614−616.
(12) Vogelstein, B.; Fearon, E. R.; Hamilton, S. R.; Kern, S. E.; Preisinger, A. C.; Leppert, M.; Nakamura, Y.; White, R.; Smits, A. M.; Bos, J. L. Genetic alterations during colorectal-tumor development. *N. Engl. J. Med.* **1988**, *319*, 525−532.
(13) Baker, S. J.; Fearon, E. R.; Nigro, J. M.; Hamilton, S. R.; Preisinger, A. C.; Jessup, J. M.; vanTuinen, P.; Ledbetter, D. H.; Barker, D. F.; Nakamura, Y.; White, R.; Vogelstein, B. Chromosome 17 deletions and p53 gene mutations in colorectal carcinomas. *Science* **1989**, *244*, 217−221.
(14) Wood, L. D.; Parsons, D. W.; Jones, S.; Lin, J.; Sjoblom, T.; Leary, R. J.; Shen, D.; Boca, S. M.; Barber, T.; Ptak, J.; Silliman, N.; Szabo, S.; Dezso, Z.; Ustyanksky, V.; Nikolskaya, T.; Nikolsky, Y.; Karchin, R.; Wilson, P. A.; Kaminker, J. S.; Zhang, Z.; Croshaw, R.; Willis, J.; Dawson, D.; Shipitsin, M.; Willson, J. K.; Sukumar, S.; Polyak, K.; Park, B. H.; Pethiyagoda, C. L.; Pant, P. V.; Ballinger, D. G.; Sparks, A. B.; Hartigan, J.; Smith, D. R.; Suh, E.; Papadopoulos, N.; Buckhaults, P.; Markowitz, S. D.; Parmigiani, G.; Kinzler, K. W.; Velculescu, V. E.; Vogelstein, B. The genomic landscapes of human breast and colorectal cancers. *Science* **2007**, *318*, 1108−1113.
(15) Jimenez, C. R.; Knol, J. C.; Meijer, G. A.; Fijneman, R. J. Proteomics of colorectal cancer: overview of discovery studies and identification of commonly identified cancer-associated proteins and candidate CRC serum markers. *J. Proteomics* **2010**, *73*, 1873−1895.
(16) Wisniewski, J. R.; Ostasiewicz, P.; Dus, K.; Zielinska, D. F.; Gnad, F.; Mann, M. Extensive quantitative remodeling of the proteome between normal colon tissue and adenocarcinoma. *Mol. Syst. Biol.* **2012**, *8*, 611.
(17) Zhang, B.; Wang, J.; Wang, X.; Zhu, J.; Liu, Q.; Shi, Z.; Chambers, M. C.; Zimmerman, L. J.; Shaddox, K. F.; Kim, S.; Davies, S. R.; Wang, S.; Wang, P.; Kinsinger, C. R.; Rivers, R. C.; Rodriguez, H.; Townsend, R. R.; Ellis, M. J.; Carr, S. A.; Tabb, D. L.; Coffey, R. J.; Slebos, R. J.; Liebler, D. C.; Nci, C. Proteogenomic characterization of human colon and rectal cancer. *Nature* **2014**, *513*, 382−387.
(18) Uzozie, A.; Nanni, P.; Staiano, T.; Grossmann, J.; Barkow-Oesterreicher, S.; Shay, J. W.; Tiwari, A.; Buffoli, F.; Laczko, E.; Marra, G. Sorbitol dehydrogenase overexpression and other aspects of dysregulated protein expression in human precancerous colorectal neoplasms: a quantitative proteomics study. *Mol. Cell. Proteomics* **2014**, *13*, 1198−1218.
(19) Wisniewski, J. R.; Ostasiewicz, P.; Mann, M. High recovery FASP applied to the proteomic analysis of microdissected formalin fixed paraffin embedded cancer tissues retrieves known colon cancer markers. *J. Proteome Res.* **2011**, *10*, 3040−3049.
(20) Wisniewski, J. R. Proteomic sample preparation from formalin fixed and paraffin embedded tissue. *J. Visualized Exp.* **2013**, DOI: 10.3791/50589.
(21) Wisniewski, J. R.; Gaugaz, F. Z. Fast and sensitive total protein and Peptide assays for proteomic analysis. *Anal. Chem.* **2015**, *87*, 4110−4116.
(22) Wisniewski, J. R.; Mann, M. Consecutive proteolytic digestion in an enzyme reactor increases depth of proteomic and phosphoproteomic analysis. *Anal. Chem.* **2012**, *84*, 2631−2637.
(23) Wisniewski, J. R.; Zielinska, D. F.; Mann, M. Comparison of ultrafiltration units for proteomic and N-glycoproteomic analysis by the filter-aided sample preparation method. *Anal. Biochem.* **2011**, *410*, 307−309.
(24) Olsen, J. V.; Macek, B.; Lange, O.; Makarov, A.; Horning, S.; Mann, M. Higher-energy C-trap dissociation for peptide modification analysis. *Nat. Methods* **2007**, *4*, 709−712.
(25) Cox, J.; Mann, M. MaxQuant enables high peptide identification rates, individualized p.p.b.-range mass accuracies and proteome-wide protein quantification. *Nat. Biotechnol.* **2008**, *26*, 1367−1372.
(26) Cox, J.; Neuhauser, N.; Michalski, A.; Scheltema, R. A.; Olsen, J. V.; Mann, M. Andromeda: A Peptide Search Engine Integrated into the MaxQuant Environment. *J. Proteome Res.* **2011**, *10*, 1794.
(27) Cox, J.; Hein, M. Y.; Luber, C. A.; Paron, I.; Nagaraj, N.; Mann, M. Accurate proteome-wide label-free quantification by delayed normalization and maximal peptide ratio extraction, termed MaxLFQ. *Mol. Cell. Proteomics* **2014**, *13*, 2513−2526.
(28) Benjamini, Y.; Hochberg, Y. Controlling the False Discovery rate: A Practical and Powerful Aproach to Multiple Testing. *J. R. Stat. Soc.* **1995**, *57*, 289−300.
(29) Wisniewski, J. R.; Rakus, D. Multi-enzyme digestion FASP and the 'Total Protein Approach'-based absolute quantification of the Escherichia coli proteome. *J. Proteomics* **2014**, *109C*, 322−331.
(30) Wisniewski, J. R.; Hein, M. Y.; Cox, J.; Mann, M. A 'proteomic ruler' for protein copy number and concentration estimation without spike-in standards. *Mol. Cell. Proteomics* **2014**, *13*, 3497.
(31) Wisniewski, J. R.; Gizak, A.; Rakus, D. Integrating Proteomics and Enzyme Kinetics Reveals Tissue-Specific Types of the Glycolytic and Gluconeogenic Pathways. *J. Proteome Res.* **2015**, *14*, 3263.
(32) Rakus, D.; Gizak, A.; Deshmukh, A.; Wisniewski, J. R. Absolute quantitative profiling of the key metabolic pathways in slow and fast skeletal muscle. *J. Proteome Res.* **2015**, *14*, 1400−1411.
(33) Wisniewski, J. R.; Koepsell, H.; Gizak, A.; Rakus, D. Absolute protein quantification allows differentiation of cell-specific metabolic routes and functions. *Proteomics* **2015**, *15*, 1316−1325.
(34) Wisniewski, J. R.; Dus, K.; Mann, M. Proteomic workflow for analysis of archival formalin-fixed and paraffin-embedded clinical samples to a depth of 10 000 proteins. *Proteomics: Clin. Appl.* **2013**, *7*, 225−233.
(35) Derenzini, M.; Montanaro, L.; Trere, D. What the nucleolus says to a tumour pathologist. *Histopathology* **2009**, *54*, 753−762.
(36) Ori, A.; Banterle, N.; Iskar, M.; Andres-Pons, A.; Escher, C.; Khanh Bui, H.; Sparks, L.; Solis-Mezarino, V.; Rinner, O.; Bork, P.; Lemke, E. A.; Beck, M. Cell type-specific nuclear pores: a case in point for context-dependent stoichiometry of molecular machines. *Mol. Syst. Biol.* **2013**, *9*, 648.
(37) Wisniewski, J. R.; Schwanbeck, R. High mobility group I/Y: multifunctional chromosomal proteins causally involved in tumor progression and malignant transformation (review). *Int. J. Mol. Med.* **2000**, *6*, 409−419.
(38) Sgarra, R.; Rustighi, A.; Tessari, M. A.; Di Bernardo, J.; Altamura, S.; Fusco, A.; Manfioletti, G.; Giancotti, V. Nuclear phosphoproteins HMGA and their relationship with chromatin structure and cancer. *FEBS Lett.* **2004**, *574*, 1−8.
(39) Hanahan, D.; Weinberg, R. A. Hallmarks of cancer: the next generation. *Cell* **2011**, *144*, 646−674.
(40) Vashee, S.; Simancek, P.; Challberg, M. D.; Kelly, T. J. Assembly of the human origin recognition complex. *J. Biol. Chem.* **2001**, *276*, 26666−26673.
(41) Heitzer, E.; Tomlinson, I. Replicative DNA polymerase mutations in cancer. *Curr. Opin. Genet. Dev.* **2014**, *24*, 107−113.
(42) Kimura, H.; Tao, Y.; Roeder, R. G.; Cook, P. R. Quantitation of RNA polymerase II and its transcription factors in an HeLa cell: little soluble holoenzyme but significant amounts of polymerases attached to the nuclear substructure. *Mol. Cell. Biol.* **1999**, *19*, 5383−5392.
(43) Jackson, D. A.; Iborra, F. J.; Manders, E. M.; Cook, P. R. Numbers and organization of RNA polymerases, nascent transcripts, and transcription units in HeLa nuclei. *Molecular biology of the cell* **1998**, *9*, 1523−1536.
(44) Pombo, A.; Jackson, D. A.; Hollinshead, M.; Wang, Z.; Roeder, R. G.; Cook, P. R. Regional specialization in human nuclei: visualization of discrete sites of transcription by RNA polymerase III. *EMBO journal* **1999**, *18*, 2241−2253.
(45) Gatenby, R. A.; Gillies, R. J. Why do cancers have high aerobic glycolysis? *Nat. Rev. Cancer* **2004**, *4*, 891−899.
(46) Vander Heiden, M. G.; Cantley, L. C.; Thompson, C. B. Understanding the Warburg effect: the metabolic requirements of cell proliferation. *Science* **2009**, *324*, 1029−1033.
(47) Warburg, O. On respiratory impairment in cancer cells. *Science* **1956**, *124*, 269−270.
(48) Altenberg, B.; Greulich, K. O. Genes of glycolysis are ubiquitously overexpressed in 24 cancer classes. *Genomics* **2004**, *84*, 1014−1020.
(49) Bi, X.; Lin, Q.; Foo, T. W.; Joshi, S.; You, T.; Shen, H. M.; Ong, C. N.; Cheah, P. Y.; Eu, K. W.; Hew, C. L. Proteomic analysis of colorectal

DOI: 10.1021/acs.jproteome.5b00523
J. Proteome Res. 2015, 14, 4005−4018

cancer reveals alterations in metabolic pathways: mechanism of tumorigenesis. *Mol. Cell. Proteomics* **2006**, *5*, 1119−1130.
(50) Roth, U.; Razawi, H.; Hommer, J.; Engelmann, K.; Schwientek, T.; Muller, S.; Baldus, S. E.; Patsos, G.; Corfield, A. P.; Paraskeva, C.; Hanisch, F. G. Differential expression proteomics of human colorectal cancer based on a syngeneic cellular model for the progression of adenoma to carcinoma. *Proteomics* **2010**, *10*, 194−202.
(51) Lu, B.; Xu, J.; Lai, M.; Zhang, H.; Chen, J. A transcriptome anatomy of human colorectal cancers. *BMC Cancer* **2006**, *6*, 40.
(52) Patra, K. C.; Wang, Q.; Bhaskar, P. T.; Miller, L.; Wang, Z.; Wheaton, W.; Chandel, N.; Laakso, M.; Muller, W. J.; Allen, E. L.; Jha, A. K.; Smolen, G. A.; Clasquin, M. F.; Robey, R. B.; Hay, N. Hexokinase 2 is required for tumor initiation and maintenance and its systemic deletion is therapeutic in mouse models of cancer. *Cancer Cell* **2013**, *24*, 213−228.
(53) Haber, R. S.; Rathan, A.; Weiser, K. R.; Pritsker, A.; Itzkowitz, S. H.; Bodian, C.; Slater, G.; Weiss, A.; Burstein, D. E. GLUT1 glucose transporter expression in colorectal carcinoma: a marker for poor prognosis. *Cancer* **1998**, *83*, 34−40.
(54) Liu, X.; Wang, X.; Zhang, J.; Lam, E. K.; Shin, V. Y.; Cheng, A. S.; Yu, J.; Chan, F. K.; Sung, J. J.; Jin, H. C. Warburg effect revisited: an epigenetic link between glycolysis and gastric carcinogenesis. *Oncogene* **2010**, *29*, 442−450.
(55) Dong, C.; Yuan, T.; Wu, Y.; Wang, Y.; Fan, T. W.; Miriyala, S.; Lin, Y.; Yao, J.; Shi, J.; Kang, T.; Lorkiewicz, P.; St Clair, D.; Hung, M. C.; Evers, B. M.; Zhou, B. P. Loss of FBP1 by Snail-mediated repression provides metabolic advantages in basal-like breast cancer. *Cancer Cell* **2013**, *23*, 316−331.
(56) Chen, M.; Zhang, J.; Li, N.; Qian, Z.; Zhu, M.; Li, Q.; Zheng, J.; Wang, X.; Shi, G. Promoter hypermethylation mediated downregulation of FBP1 in human hepatocellular carcinoma and colon cancer. *PLoS One* **2011**, *6*, e25564.
(57) Li, H.; Wang, J.; Xu, H.; Xing, R.; Pan, Y.; Li, W.; Cui, J.; Zhang, H.; Lu, Y. Decreased fructose-1,6-bisphosphatase-2 expression promotes glycolysis and growth in gastric cancer cells. *Mol. Cancer* **2013**, *12*, 110.
(58) Li, B.; Qiu, B.; Lee, D. S.; Walton, Z. E.; Ochocki, J. D.; Mathew, L. K.; Mancuso, A.; Gade, T. P.; Keith, B.; Nissim, I.; Simon, M. C. Fructose-1,6-bisphosphatase opposes renal carcinoma progression. *Nature* **2014**, *513*, 251−255.
(59) Alderton, G. K. Tumorigenesis: FBP1 is suppressed in kidney tumours. *Nat. Rev. Cancer* **2014**, *14*, 575.
(60) Prothmann, C.; Wellard, J.; Berger, J.; Hamprecht, B.; Verleysdonk, S. Primary cultures as a model for studying ependymal functions: glycogen metabolism in ependymal cells. *Brain Res.* **2001**, *920*, 74−83.
(61) Mestres, P.; Diener, M.; Rummel, W. Storage of glycogen in rat colonic epithelium during induction of secretion and absorption in vitro. *Cell Tissue Res.* **1990**, *261*, 195−203.
(62) Rousset, M.; Zweibaum, A.; Fogh, J. Presence of glycogen and growth-related variations in 58 cultured human tumor cell lines of various tissue origins. Presence and cell growth-related variations of glycogen in human colorectal adenocarcinoma cell lines in culture. *Cancer Res.* **1981**, *41*, 1165−1170.
(63) Rousset, M.; Chevalier, G.; Rousset, J. P.; Dussaulx, E.; Zweibaum, A. Presence and cell growth-related variations of glycogen in human colorectal adenocarcinoma cell lines in culture. *Cancer Res.* **1979**, *39*, 531−534.
(64) Frederiks, W. M.; Vizan, P.; Bosch, K. S.; Vreeling-Sindelarova, H.; Boren, J.; Cascante, M. Elevated activity of the oxidative and non-oxidative pentose phosphate pathway in (pre)neoplastic lesions in rat liver. *Int. J. Exp. Pathol.* **2008**, *89*, 232−240.
(65) Langbein, S.; Zerilli, M.; Zur Hausen, A.; Staiger, W.; Rensch-Boschert, K.; Lukan, N.; Popa, J.; Ternullo, M. P.; Steidler, A.; Weiss, C.; Grobholz, R.; Willeke, F.; Alken, P.; Stassi, G.; Schubert, P.; Coy, J. F. Expression of transketolase TKTL1 predicts colon and urothelial cancer patient survival: Warburg effect reinterpreted. *Br. J. Cancer* **2006**, *94*, 578−585.
(66) Laiho, P.; Hienonen, T.; Mecklin, J. P.; Jarvinen, H.; Karhu, A.; Launonen, V.; Aaltonen, L. A. Mutation and LOH analysis of ACO2 in colorectal cancer: no evidence of biallelic genetic inactivation. *Journal of medical genetics* **2003**, *40*, e73.
(67) Friedman, D. B.; Hill, S.; Keller, J. W.; Merchant, N. B.; Levy, S. E.; Coffey, R. J.; Caprioli, R. M. Proteome analysis of human colon cancer by two-dimensional difference gel electrophoresis and mass spectrometry. *Proteomics* **2004**, *4*, 793−811.
(68) Borger, D. R.; Tanabe, K. K.; Fan, K. C.; Lopez, H. U.; Fantin, V. R.; Straley, K. S.; Schenkein, D. P.; Hezel, A. F.; Ancukiewicz, M.; Liebman, H. M.; Kwak, E. L.; Clark, J. W.; Ryan, D. P.; Deshpande, V.; Dias-Santagata, D.; Ellisen, L. W.; Zhu, A. X.; Iafrate, A. J. Frequent mutation of isocitrate dehydrogenase (IDH)1 and IDH2 in cholangiocarcinoma identified through broad-based tumor genotyping. *Oncologist* **2012**, *17*, 72−79.
(69) Sanchez-Arago, M.; Chamorro, M.; Cuezva, J. M. Selection of cancer cells with repressed mitochondria triggers colon cancer progression. *Carcinogenesis* **2010**, *31*, 567−576.
(70) Deberardinis, R. J.; Mancuso, A.; Daikhin, E.; Nissim, I.; Yudkoff, M.; Wehrli, S.; Thompson, C. B. Beyond aerobic glycolysis: transformed cells can engage in glutamine metabolism that exceeds the requirement for protein and nucleotide synthesis. *Proc. Natl. Acad. Sci. U. S. A.* **2007**, *104*, 19345−19350.
(71) Deberardinis, R. J.; Sayed, N.; Ditsworth, D.; Thompson, C. B. Brick by brick: metabolism and tumor cell growth. *Curr. Opin. Genet. Dev.* **2008**, *18*, 54−61.
(72) Fan, J.; Kamphorst, J. J.; Mathew, R.; Chung, M. K.; White, E.; Shlomi, T.; Rabinowitz, J. D. Glutamine-driven oxidative phosphorylation is a major ATP source in transformed mammalian cells in both normoxia and hypoxia. *Mol. Syst. Biol.* **2013**, *9*, 712.
(73) Currie, E.; Schulze, A.; Zechner, R.; Walther, T. C.; Farese, R. V., Jr. Cellular fatty acid metabolism and cancer. *Cell Metab.* **2013**, *18*, 153−161.
(74) Glatz, J. F. Lipids and lipid binding proteins: A perfect match. *Prostaglandins, Leukotrienes Essent. Fatty Acids* **2014**, *93*, 45.
(75) Cao, Y.; Pearman, A. T.; Zimmerman, G. A.; McIntyre, T. M.; Prescott, S. M. Intracellular unesterified arachidonic acid signals apoptosis. *Proc. Natl. Acad. Sci. U. S. A.* **2000**, *97*, 11280−11285.
(76) Nagaraj, N.; Wisniewski, J. R.; Geiger, T.; Cox, J.; Kircher, M.; Kelso, J.; Paabo, S.; Mann, M. Deep proteome and transcriptome mapping of a human cancer cell line. *Mol. Syst. Biol.* **2011**, *7*, 548.
(77) Vizcaino, J. A.; Deutsch, E. W.; Wang, R.; Csordas, A.; Reisinger, F.; Rios, D.; Dianes, J. A.; Sun, Z.; Farrah, T.; Bandeira, N.; Binz, P. A.; Xenarios, I.; Eisenacher, M.; Mayer, G.; Gatto, L.; Campos, A.; Chalkley, R. J.; Kraus, H. J.; Albar, J. P.; Martinez-Bartolome, S.; Apweiler, R.; Omenn, G. S.; Martens, L.; Jones, A. R.; Hermjakob, H. ProteomeXchange provides globally coordinated proteomics data submission and dissemination. *Nat. Biotechnol.* **2014**, *32*, 223−226.

DOI: 10.1021/acs.jproteome.5b00523
J. Proteome Res. 2015, 14, 4005−4018